Meas. Sci. Technol. **16** (2005) 1157–1169 doi:10.1088/0957-0233/16/5/016

The analysis of physical background of tree sap flow measurement based on thermal methods

Fyodor A Tatarinov[1,4], Jiri Kučera[2] and Emil Cienciala[3]

[1] Institute of Ecology and Evolution, Russian Academy of Science, Leninsky pr. 33, Moscow, Russia
[2] Environmental Measuring Systems, Turisticka 5, Brno, Czech Republic
[3] IFER—Institute of Forest Ecosystem Research, 25401 Jílové u Prahy 1544, Czech Republic

E-mail: fedor.tatarinov@ifer.cz

Received 15 April 2004, in final form 1 February 2005
Published 30 March 2005
Online at stacks.iop.org/MST/16/1157

Abstract
The underlying physics of three specific thermal methods to measure tree sap flow was investigated. All these methods utilize local heating and measure heat dissipation caused by moving water. The application of heating was specific for each of the methods tested, herewith distinguishing the following alternatives: (1) thin needle perpendicular to stem surface, (2) rectangular plate directed vertically towards stem axis and (3) constrained volume. For all alternatives, sap flow volume can basically be estimated from the observed temperature change and applied energy. The original equations applicable for some of these methods were derived either empirically (Granier 1985 *Ann. For. Sci.* **42** 193–200) or from simplified heat balance equations (Cermak *et al* 1973 *Biol. Plant.* **15** 171–8). The aim of this study was to rigorously verify these particular methods by a detailed physical analysis, using a numerical solution of the heat conductivity equation in a three-dimensional coordinate system. The analysis showed that the dependence of sap flow on wood temperature in a certain point inside the heated domain could be satisfactorily approximated ($r^2 \geqslant 0.99$) by specific curves of hyperbolic type for all three considered configurations of heating. However, the sensitivity of this dependence to uncertainty factors (wood heat conductivity, non-homogeneity of sap flow radial profile and external temperature gradients) was strongly affected by the size of the heated domain. In general, the sensitivity of the temperature field in wood to all uncertainty factors decreased with increasing volume of the heated domain. Thus, the sap flow sensor based on needle heating was most sensitive to uncertainty factors, whereas the volume heating showed a relatively stable temperature field. The simple heat balance model applied for the restricted volume approach (Kučera *et al* 1977 *Biol. Plant. (Praha)* **19** 413–20) proved to be a satisfactory approximation for the volume heating method.

Keywords: sap flow measurement, heat transfer, thermal methods, wood properties

(Some figures in this article are in colour only in the electronic version)

[4] Present address: IFER—Institute of Forest Ecosystem Research, 25401 Jílové u Prahy 1544, Czech Republic.

1. Introduction

The measurement of water use by plants, especially by trees, is needed for many purposes in forestry, ecology, hydrology and microclimatology. This is why several methods for field measurement of the ascending water flow (sap flow[5]) through a plant stem (or branch) cross-section have been elaborated during the last 30 years (Cermak *et al* 1973, 1982, 1991, Kučera *et al* 1977, Sakuratani 1981, Granier 1985, Swanson 1967, 1994).

1.1. Physical basis of thermal methods

All methods commonly applied for sap flow measurement are based on the same physical principle. A certain part of conductive woody tissue is heated and heat dissipation is assessed from temperature measurements in two locations of the plant stem (or branch), namely in the heated domain and outside the heated domain.

It is important to distinguish yet another group of thermal methods. These are aimed at measuring linear velocity of ascending water applying heating in a form of heat pulse (the so-called heat pulse technique). The velocity of ascending water is then derived from the time when the applied heat pulse reaches certain point(s) outside the heater (Huber and Schmidt 1936, Swanson 1967). The main advantage of pulse heating is that no reference temperature is required, so that the influence of the ambient temperature gradients or that from wood heterogeneity is minimized. The limiting factors of this method are the time required for reaching a steady state after switching the heating off and the estimation of wound diameter and xylem properties (Kostner *et al* 1998). In contrast, the constant heating approaches represent a truly continuous measurement, but they require a reference temperature to be measured, which can be a source of errors if the conditions of ambient wood in the reference point differ from those of the heated domain. Additionally, the constant heating requires higher power consumption.

The methods aiming at volumetric assessment of water mass flow, which is the subject of this study, usually apply a constant heating generating a quasi-steady-state temperature field. The heat flux outwards from the heated domain (zone) consists of two parts: heat loss by thermal conductivity and heat convection by moving water. The heat loss by water movement is proportional to water mass flow: under constant heating a higher temperature in the heated zone corresponds to a lower sap flux and vice versa. Today, there are two commonly used methods of this type providing the measurement of sap flow in large stems. The first one, the so-called tissue heat balance (THB) method (Cermak *et al* 1973, 1982, 1991, Kučera *et al* 1977), is based on a volume (three-dimensional (3D)) heating of stem segment. The second one, called the heat dissipation technique (HDT, Granier (1985)), is based on the heating by a needle (one-dimensional heating). Although both methods have been used in many ecological studies all over the world, their physical basis has not been adequately described yet. Kučera *et al* (1977) related sap flux (Q_W defined as the mass of water passing through a defined area of stem cross-section per unit of time) to the measured temperature difference between the heated wood and a control location (ΔT) by an ordinary differential equation assuming the temperature field within the heated volume to be homogeneous. Granier (1985) based his approach on an empirically derived dependence between Q_W and ΔT. Several authors noticed a disagreement between the results obtained by these methods when applied to the same sample trees (Kostner *et al* 1998, Lundblad *et al* 2001, Schubert 1999, Clearwater *et al* 1999).

The aim of this study was to (1) set up a physical formulation of estimation of three-dimensional temperature field in wood for different space distributions of heat input taking Q_W as parameter, (2) provide a solution of this task, (3) analyse the sensitivity of the obtained temperature field in a steady state to likely uncertainty factors, (4) verify the results by field and laboratory experiments and (5) evaluate advantages and disadvantages of each heat input scheme.

1.2. Properties of wood from the point of view of sap flow measurement

There are two main types of liquid flows along the tree stem: (1) upward sap (xylem) flow of water with dissolved nutrients from roots up to crown and (2) downward phloem flow of photosynthesis products. Phloem is a living tissue forming a thin layer (about 1 mm) located between bark and woody xylem tissues. Sap flow takes place in the conductive xylem tissues (sapwood), located in the outer part of the stem cross-sectional area. Sapwood is usually more than one order thicker as compared to phloem (Zimmerman 1983). Whereas the linear velocities of phloem and xylem flows may be comparable (Rokitta *et al* 2003), the volumetric flow in phloem is negligible relative to volume transported via xylem conductive area. Hence, this paper is focused exclusively on the measurement of sap flow.

The sap flow pattern is usually not homogeneous across the stem: its radial profile is generally asymmetric with one maximum in the outer part of the sapwood (Cermak *et al* 1992, Phillips *et al* 1996). The total width of the sap flow zone can be from several millimetres up to the whole stem radius. In the temperate climate zone, the maximum values of sap flux may reach about 0.1 kg cm^{-2} h^{-1} and the daily total sap flow per tree on a clear summer's day may reach 200 kg $tree^{-1}$ h^{-1} for deciduous and about 100 kg $tree^{-1}$ h^{-1} for coniferous species. The corresponding linear velocities of water range from 1 to 30 m h^{-1} (Cermak *et al* 1992).

Wood may be considered as a two-phase medium composed of a solid fraction (cellulose) forming the vessel walls and a sap liquid filling the free space. Due to only a fractional concentration of dissolved nutrients, sap may safely be considered and treated as pure water. This medium is significantly anisotropic: (1) the significant water flow takes place only in one direction along the conductive tissues and (2) the heat conductivity of wood is significantly (up to 2.5 times) higher along than across the conductive tissues (Steinhagen 1977, Siau 1984). The heat conductivity increases with wood

[5] Sap flow is a biological term that describes water passing through conductive xylem of tree stems or branches. It is commonly expressed in unit volume per unit of stem circumference that is rescaled to a whole tree if needed. Once related to specific area (i.e., stem segment, conductive part of stem or entire cross-sectional area of tree stem or branch) it is called sap flux (water flux quantity per unit area) instead. In this study, the term sap flow always describes the volume of ascending sap.

moisture and wood density. The typical values of wood heat conductivity across the conductive tissues range between 0.15 and 0.40 W m^{-1} K^{-1} (Steinhagen 1977).

The mass flow rate at a given point of tree stem results from three factors: (1) linear velocity of water, (2) water content of wood and (3) proportion of moving and immobile water. However, the linear velocity of water in individual conductive cells basically depends on the fourth power of their diameter according to the Hagen–Poiseuille law (Zimmerman 1983).

1.3. Effect of uncertainty factors

When estimating stem sap flow from temperature field in woody tissue, several possible uncertainty factors should be considered, notably variation of sap flow in the radial direction, natural temperature gradients in the measured domain of stem and heterogeneity of wood properties.

If sap flow varies along the radius within the heated domain, the heat loss by water flux, and consequently the temperature pattern, is not homogeneous along the stem radius. Consequently, the correct estimation of total stem sap flow requires measurement of the whole radial temperature profile.

A woody stem may exhibit significant temperature gradients, both in the vertical (along stem axis) and radial directions (towards stem axis). The latter, originating from diurnal fluctuations of ambient temperature buffered by actual heat conductivity of wood (Herrington 1969), is the most important (although often neglected), reaching up to 1 K cm^{-1}. A body with a high heat conductivity inserted into the wood (such as heating or sensing element) can function as a 'short circuit' for heat, homogenizing these gradients and consequently establishing a different temperature profile as compared to that in surrounding wood. This may introduce an error when measuring wood temperature. The vertical gradient can evoke an error of measurement because the reference sensing element placed below the heated volume could be in different ambient conditions from the heated sensing element. The vertical gradient is most significant when measurement is performed close to the ground surface (Kostner *et al* 1998).

Wood properties are often not homogeneous, especially along the stem radius. Some tree species have a dry heartwood (middle part of stem cross-sectional area, non-conductive tissues), whereas others are moist across the whole profile. Consequently, heat conductivity can be variable along the stem radius. Moreover, the extent of the moist part of tree stem offers generally no useful approximation of the conductive area of the stem. Therefore, the estimation of the conductive profile is an independent and complicated task.

It is important to realize that sap flow measurements are performed in living organisms, which should be basically unaffected by the method to allow long-term undisturbed measurements and observation. Hence, any potential disturbance by excess temperature and tissue damage by sensors and heaters must be minimized to the largest possible extent. Generally said, the measuring arrangement optimal from the technical point of view might be fatal for the measured plant. In practice, only a limited amount of interfering foreign bodies may be inserted into conductive tissues and their size is an extremely important factor, too.

2. Material and methods

2.1. The mathematical problem definition

The density of internal energy in wood is described by the following equation,

$$c_v \frac{\partial T}{\partial t} = q(\mathbf{x}, t) + j(\mathbf{x}, t) + P(\mathbf{x}, t) \qquad (1)$$

where T is the temperature, c_v is the specific heat of wood per unit volume, the terms of the right-hand side are the contribution of heat conductivity, $q(\mathbf{x}, t)$, the convective heat flux caused by moving water, $j(\mathbf{x}, t)$, and the power input, $P(\mathbf{x}, t)$. Let us consider wood as a continuous medium consisting of two phases: immobile and movable. Consequently, $c_v = \rho_w c_w + \rho_x c_x$, where ρ_w, ρ_x, c_w and c_x are the densities and specific heats of water and xylem. When taking into account the anisotropy of wood the conductivity heat flux can be written as $q(\mathbf{x}, t) = \nabla(\boldsymbol{\lambda}_W \nabla T)$, where the symbol ∇ (nabla) means the vector, the components of which are derivatives on the corresponding coordinate axes: $\nabla = \left\{\frac{\partial}{\partial x_1}, \frac{\partial}{\partial x_2}, \frac{\partial}{\partial x_3}\right\}$. The convective heat flux can be written as $j(\mathbf{x}, t) = -\rho_w \beta \cdot c_w(\mathbf{v}\nabla)T$, where $\mathbf{v}$ is the sap flow velocity, $\boldsymbol{\lambda}_W$ is the tensor of heat conductivity of moist wood, and β is the portion of moving water in the total water content $(0 \leqslant \beta \leqslant 1)$.

Consequently, equation (1) can be written as follows:

$$(\rho_w c_w + \rho_x c_x)\frac{\partial T}{\partial t} = \nabla(\boldsymbol{\lambda}_W \nabla T) - \rho_w \beta \cdot c_w(\mathbf{v}\nabla)T + P(\mathbf{x}, t) \qquad (2)$$

The temperature field in a measuring element supposing isotropic heat conductivity of its material can be described by a simple equation of heat conductivity,

$$\rho_h \cdot c_h \frac{\partial T}{\partial t} = P(\mathbf{x}, t) + \lambda_h \nabla^2 T \qquad (3)$$

where λ_h, ρ_h and c_h are the heat conductivity, density and specific heat of measuring element. Usually, $\lambda_h \gg |\boldsymbol{\lambda}_W|$.

The entire analysis and simulations are based on these very general equations. Further, instead of water velocity $\mathbf{v}$ we apply the water mass flow $\mathbf{Q}_W = \mathbf{v} \cdot \beta \cdot \rho_w$, which is our target product. We considered the following arrangements of power input:

(1) Homogeneous heating by a one-dimensional (needle) segment perpendicular to the stem surface—further referenced as needle heating.
(2) Homogeneous heating by a two-dimensional rectangular segment inserted vertically perpendicular to stem surface—plate heating.
(3) Homogeneous heating in a three-dimensional rectangular block—volumetric heating.

2.2. Analytical solution using Green's function

Equation (2) for homogeneous media in the non-limited n-dimensional space has the following analytical solution,

$$T(\mathbf{x}, t) = T_0(\mathbf{x}, t) + \int \mathrm{d}t'\, \mathrm{d}^n\mathbf{x}'\, G_R(\mathbf{x} - \mathbf{x}', t - t')P(t', \mathbf{x}') \qquad (4)$$

where $T_0(\mathbf{x}, t)$ is an arbitrary solution of homogeneous equation (2) (with $P(\mathbf{x}, t) \equiv 0$), Green's function $G_R(\mathbf{x}, t)$ has the form

$$G_R(\mathbf{x}, t) = \frac{1}{a_1} \prod_{i=1}^{n} \sqrt{\frac{a_1}{4\pi\lambda_i t}} \times \exp\left(-\sum_{i=1}^{n} \frac{(Q_{W,i} c_w t - a_1 x_i)^2}{4\lambda_i a_1 t}\right) \tag{5}$$

for $t > 0$ and $G_R(\mathbf{x}, t) = 0$ for $t \leqslant 0$, where $t = 0$ is the moment of the start of heating, λ_i, $i = 1, \ldots, n$, is the ith diagonal element of the tensor of heat conductivity $\boldsymbol{\lambda}_W$, i.e. heat conductivity in direction i and $a_1 = c_w \cdot \rho_w + c_x \cdot \rho_x$.

Further, we suppose the following additional conditions as default:

(a) Sap flow vector $\mathbf{Q}_W$ is directed vertically (i.e., along the z-axis) in the whole considered volume. Thus, only its z-coordinate will be non-zero. Further, Q_W will mean $|\mathbf{Q}_W| = Q_{W,z}$.
(b) $T_0(\mathbf{x}, t) = T_0 \equiv 0$; we will consider $\Delta T(\mathbf{x}, t) = T(\mathbf{x}, t) - T_0$ instead of $T(\mathbf{x}, t)$.
(c) The values of wood heat conductivity along (λ_z) and across (λ_x) vessels are proportional: $\lambda_z = 2.5\lambda_x$.
(d) As we are primarily interested in the basic analysis and comparison of different types of sensors and not the precise prediction of actual temperature field for concrete tree stems, we assume that the sample stem is thick enough to consider its surface as locally flat. This condition allows us to consider the heating in the half-limited three-dimensional space with Cartesian coordinate system $\mathbf{x} = (x, z, r)$, where x is tangential, z is vertical and $r \geqslant 0$ is radial direction ($r = 0$ is the stem surface and $r > 0$ is inside the stem).

Under condition (d) according to the method of reflection supposing no heat flux outside of stem the Green's function in equation (4) will be

$$\begin{aligned} G(\mathbf{x} - \mathbf{x}', t - t') &\equiv G(x - x', z - z', r - r', t - t') \\ &= G_R(x - x', z - z', r - r', t - t') \\ &\quad + G_R(x - x', z - z', r + r', t - t'), \end{aligned} \tag{6}$$

where G_R is given by equation (5).

In the case of needle heating the analytical integration of (6) is possible under some simplifications. Let us consider the needle heating in a two-dimensional Cartesian coordinate system (the vertical, z, and tangential, x, directions). This approximation supposes (a) radially homogeneous sap flow within the depth of the needle and (b) no significant heat fluxes in the radial direction. Since in the given case $P(t, \mathbf{x}) = P(t)\delta(\mathbf{x})$, equation (4) will take the form

$$T(\mathbf{x}, t) = T_0(x, z) + \int \frac{1}{4\pi\sqrt{\lambda_x\lambda_z}(t - t')} \times \exp\left(-\frac{(Q_w c_w (t - t') - a_1 z)^2/\lambda_z + a_1^2 x^2/\lambda_x}{4a_1(t - t')}\right) P(t')\,\mathrm{d}t' \tag{7}$$

where $a_1 = c_w \cdot \rho_w + c_x \cdot \rho_x$. If $P(t) = P = \text{const}$, the analytical solution of (7) in a steady state is

$$T(x, z, \infty) = T_0(x, z) + \frac{P}{2\pi\sqrt{\lambda_x\lambda_z}} \cdot \exp\left(\frac{c_w Q_w z}{2\lambda_z}\right) \times K_0\left(\frac{c_w Q_w \sqrt{\lambda_z x^2 + \lambda_x z^2}}{2\lambda_z\sqrt{\lambda_x}}\right), \tag{8}$$

where $K_0(z)$ is the modified Bessel function of the second kind.

If $Q_W = 0$ (typical for night time) and the heating is applied during a limited time, i.e., $P(t) = P$ if $0 \leqslant t \leqslant t_{\text{pulse}}$ and $P(t) = 0$ otherwise, equation (7) will take a simple form:

$$\begin{aligned} T(0, t) &= T_0(0) + \int_0^{t_{\text{pulse}}} \frac{P\,\mathrm{d}t'}{4\pi\sqrt{\lambda_x\lambda_z}(t - t')} \\ &= T_0(0) + \frac{P}{4\pi\sqrt{\lambda_x\lambda_z}} \ln\frac{t}{t - t_{\text{pulse}}}, \qquad t > t_{\text{pulse}} \end{aligned} \tag{9}$$

Thus, when solving (9) for any $t > t_{\text{pulse}}$ the geometrical mean of λ_z and λ_x can be evaluated.

2.3. Numerical solution by difference schemes

Solution (6) can be applied for homogeneous media in a semi-limited space, i.e., when the curvature of stem surface and the effect of temperature homogenization along the heating elements themselves can be neglected.

In order to solve the problem for more general conditions, a specific program in C++ for direct numerical solution of equations (2) and (3) was written. The initial condition was always $T_0(\mathbf{x}) \equiv 0$ for any $\mathbf{x}$. The boundary condition in the wood was also $T(\mathbf{x}, t) = 0$ for any moment t.

2.4. Simulation experiments

All simulations were performed for sap flow values from 0 to 30 g cm^{-2} h^{-1}.

2.4.1. Configurations of heated domain. The temperature field for all mentioned configurations of the heated domain was estimated both by integrating the analytical solution (6) and by the numeric solution of equations (2) and (3). The analytical solution to analyse the most general properties of a given type of heating was always performed in a three-dimensional Cartesian coordinate system $\mathbf{x} = (x, z, r)$, $r \geqslant 0$ (see section 2.2) with homogeneous power distribution in one-, two- and three-dimensional segments for needle, plate and volumetric heating, respectively. The numerical solution of (2) and (3) took into consideration the high heat conductivity of heating elements and heat transfer through the bark.

The numerical solution for volumetric heating was performed in the above-described Cartesian coordinate system in a domain $0 \leqslant x \leqslant x_{\max}$ (taking into consideration the symmetry relative to the plane $x = 0$), $0 \leqslant r \leqslant r_{\max}$ (0 corresponding to the stem surface) and $z_{\min} \leqslant z \leqslant z_{\max}$. In the cases of needle and plate heaters, the numerical solution was performed in a cylindrical coordinate system with axes radius from the stem centre r, angle φ ($\varphi = 0$ along the heater) and height z. Taking into consideration the symmetry relative to the plane $\varphi = 0$, the difference scheme was solved in the 3D sector $0 \leqslant \varphi \leqslant \varphi_{\max}$, $z_{\min} \leqslant z \leqslant z_{\max}$ and $r_{\min} \leqslant r \leqslant R$ (R corresponding to the stem surface). The following boundary conditions were applied for numerical solution:

(1) $\partial \boldsymbol{q}/\partial r = 0$, where $\boldsymbol{q} = -\lambda\nabla T$ is the heat flux from the stem surface (i.e., $\lambda = 0$) and $T = T_0 = 0$ for other borders of the simulation domain—perfect insulation of stem surface.

(2) $q_r = -k_b \cdot (T(\mathbf{x}, t) - T_a)$, where q_r is the projection of vector $\boldsymbol{q}$ to the axis r, k_b is constant and $T_a = T_0 = 0$ for the stem surface and $T = T_0 = 0$ for other borders of the simulation domain—realistic insulation of stem surface.

(3) Realistic insulation with radial temperature gradient. $q_r = -k_b \cdot (T(\mathbf{x}, t) - T_a)$ for stem surface as in the last case, but $T_a \neq 0$. Other boundary conditions were: $T = 0$ for $r = R_{\min}$ and $\partial \boldsymbol{q}/\partial z = 0$ for $z = z_{\min}$, $z = z_{\max}$ and $\varphi = \varphi_{\max}$. The simulations were performed for temperature gradients $T_a - T_0$, 2 and 3 K.

2.4.2. Heating schedule. The study of temperature field in dependence on Q_W and other parameters was performed for two regimes: (1) short-term heat pulse and analysis of temperature response in *time*; (2) constant heating until reaching the steady state with the consequent analysis of temperature *space* distribution.

2.4.3. Approximation of simulation results. Since the result of any simulation experiment was ΔT values at the points of a regular three-dimensional grid for different Q_W values, a further analysis was required to obtain a usable functional dependence of sap flow on ΔT. The main goal of this process was to find the point of a feasible temperature measurement and the regression relating ΔT at this point to Q_W searching the optimal dependence as for both strength of this relationship (r^2) and the rigidity with respect to the likely disturbing factors.

The dependence $Q_W(\Delta T)$ was derived for any simulation with constant heating for a certain point usually inside the heated space (on the heating plate or needle). The different equations of hyperbolic type, where tested for this dependence, include that of

(i) Cermak *et al* (1973) and Kučera *et al* (1977) (for heated volume only)

$$Q_W = \frac{P}{c_w \cdot x_h \cdot \Delta T} - k \tag{10}$$

where c_w is the specific heat of water, x_h is the width of the heated volume and k is the constant estimated under $Q_W = 0$;

(ii) Granier (1985),

$$Q_W = a \cdot \left(\frac{\Delta T_{\max} - \Delta T}{\Delta T}\right)^b \tag{11}$$

where $\Delta T_{\max}$ is ΔT under $Q_W = 0$ and a, b are parameters; and

(iii) the proposed equation

$$Q_W = \frac{P \cdot b}{\Delta T - P \cdot c} - a \tag{12}$$

where a, b and c are parameters.

2.4.4. Analysis of the influence of variable factors on the heat field under different heaters. All the above-mentioned heating arrangements were tested for sensitivity to three main factors, usually unknown with satisfactory precision that can influence the temperature field: wood heat conductivity, radial profile of sap flow and radial ambient temperature gradient (ATG), as well as the specific heat of wood in the case of pulse heating.

The sensitivity to λ ($\partial T/\partial\lambda$) was evaluated as the ratio of ΔT change at a certain point inside the heated space (plate, needle) to the change of λ (both λ_x and λ_z proportionally)—both changes in per cent.

As mentioned in the introduction, the sap flow radial profile is usually non-homogeneous. Nevertheless, in practice, it is usually unknown and the total amount of water passing through the stem cross-section is the centre of our interest. The non-homogeneous sap flow radial profile potentially can evoke non-homogeneity of the temperature radial profile. This is why we have principally two possibilities to correctly estimate the total stem sap flow: (1) measure the radial profile of the temperature or (2) homogenize the temperature radial profile. Otherwise, if we measure the temperature at a single depth only and then we estimate the sap flow supposing its homogeneity within the depth of averaging, it is necessary to appreciate the possible error of this estimation.

The mentioned error evoked by the non-homogeneous sap flow radial profile was tested for a step-like sap flow profile: $Q_W = Q_{\max}$ for $d \leqslant d_{\max}$ and $Q_W = 0$ for $d > d_{\max}$, where $d \equiv R - r$ is the depth from the stem surface. First the simulation for the homogeneous sap flow within the whole depth of the heated space (d_h) was done and the regression equation for $Q_W(\Delta T)$ was derived for a certain point inside the heated space. Let us mark sap flow estimated under $d_{\max} = d_h$ as $Q_{W,0}$. Then the simulations with different sap flow depths $d_{\max} \leqslant d_h$ were performed and the dependence $Q_W(\Delta T)$ was derived by the same equation and for the same point as for the homogeneous sap flow. The total sap flow per unit stem circumference within the heated depth, $Q_{WS} = \int_0^{d_h} Q_W \,\mathrm{d}d$ in the given case, is $Q_W \cdot d_{\max}$. On the other hand, if we apply the equation obtained for $d_{\max} = d_h$ for the calculation of $Q_{W,0}$ and suppose the homogeneous sap flow, $Q_{WS,0} = Q_{W,0} \cdot d_h$. So, $Q_{WS} = Q_{WS,0}$ if $Q_W(\Delta T)/Q_{W,0}(\Delta T) = d_h/d_{\max}$. The error of sap flow measurement evoked by the non-homogeneous sap flow will be $(Q_{WS,0} - Q_{WS})/Q_{WS}$.

The analysis of the influence of the natural temperature gradient was done in the following way. The radial temperature gradient was simulated by the heat flow across the bark evoked by the constant temperature difference between the air and the heartwood, i.e., between the surfaces $r = R$ and $r = r_{\min}$. The simulation was done until the steady state was reached twice: with power $P = 0$ in order to obtain $T_0(\mathbf{x})$ and with $P > 0$. Then ΔT was calculated as $T - T_0$ for each point of the simulated volume.

2.5. Physical experiments

A series of physical experiments to measure the heat field around all mentioned types of heaters was performed on different tree species, under Q_W being surely zero (on freshly cut stem segments with diameter 20 to 25 cm). The temperatures were measured by fine (of diameter 0.3 mm) thermocouples inserted into the wood at different points inside and around the heated domain. The volume heating was done by two or three parallel 1 mm thick partially insulated steel electrodes with width 2.5 cm inserted into the wood to a depth 30 mm at 20 mm from each other. This space configuration was selected because a similar set-up has been applied in the existing THB sensors (e.g., Cermak *et al* (1973, 1982, 1991)).

The experiments with needle heating were specifically applied for the verification of the model (analytical solutions (8) and (9)) by the calculation of λ_z and λ_x and their further comparison with the data of Steinhagen (1977). The following two experiments were performed:

(1) The cut segment of spruce stem was heated by a 2 mm thick needle. The needle was inserted into the wood down to 4 cm, the applied power was about 0.12 W cm^{-1} of needle depth. The temperature of the needle was measured by a thermocouple mounted inside the needle 3 mm from its end. Additional temperatures were measured at a depth of 18 mm and 10, 20 and 40 mm above, below and on the sides of the needle and 150 mm from the needle as a reference one. The heating was applied until the steady state was reached, then the obtained temperature distribution was compared with the temperature distribution calculated using equation (6) under $Q_W = 0$ and for a range of λ_z and λ_x.

(2) The same experiment was repeated with heating lasting only 60 s. The needle temperature was measured every 3 s. Heat conductivity was obtained from the measured ΔT values according to equation (9).

3. Result and discussion

3.1. Properties of analytical solution

Equation (6) shows that under homogeneous power distribution $\Delta T = T_0 - T(\mathbf{x}, t)$ will be proportional to the power P. In general, for any power distribution, increasing $P(\mathbf{x})$ k times at any point $\mathbf{x}$, will increase $\Delta T(\mathbf{x}, t)$ k times for any $\mathbf{x}$ and t.

For needle heating, equation (8) gives the infinite values for $Q_W = 0$ and for $z = x = 0$ under any Q_W, which results from the two-dimensional approximation. Consequently under $Q_W > 0$, $\lim_{|\mathbf{x}|\to 0} |\nabla T| = \infty$, i.e., the temperature gradient close to the needle will be very high. This result is validated by the simulation experiments with a 3D model.

3.2. Simulation experiments with short-term (pulse) heating

Typical time curves of temperature in the centre of heating volume/segment $\Delta T(\mathbf{x}_0, Q_W, t)$ for different Q_W under short-term (pulse) heating are presented in figure 1(*a*). The sensitivity of $\Delta T(\mathbf{x}_0, Q_W, t)$ to Q_W dramatically varies depending on Q_W and time (figure 1(*b*)). $\mathrm{d}T/\mathrm{d}Q_W$ increases with time while the heating goes on, being higher for higher Q_W. It reaches a maximum at the end of heating and then gradually decreases, with a larger decline for a larger Q_W. The difference between ΔT values at the same time and different Q_W remains relatively small during the first minute of heating: for heating by needle the ratios $\Delta T(\mathbf{x}_0, 0, t)/\Delta T(\mathbf{x}_0, Q_{\max}, t)$, where $Q_{\max} = 30$ g cm^{-2} h^{-1}, were 1.07, 1.12 and 1.20 for time $t = 10$, 30 and 60 s, respectively. The same ratios for homogeneous heating in 1 cm^3 were 1.0, 1.07 and 1.19, respectively. This means that heating should be applied over a longer period in order to safely detect the changes in sap flow rate (i.e., in practice it should approach the steady state). It also means that a long period of cooling is required to repeat the experiment. This has a severe implication for a practical use of the impulse heating.

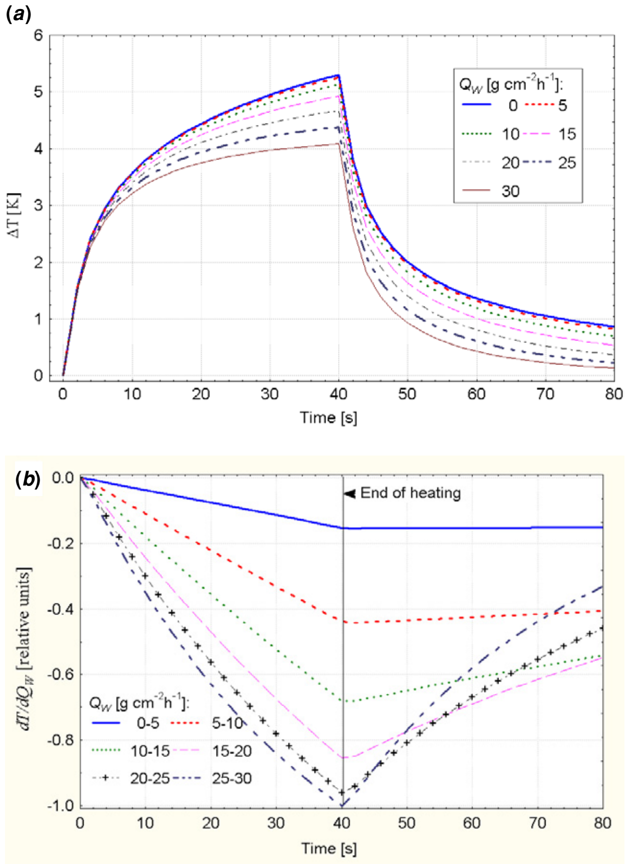

Figure 1. Pulse heating by a needle heater. Typical time dependence of needle temperature (*a*) and $\mathrm{d}\Delta T/\mathrm{d}Q_W$ under different Q_W (*b*).

The influence of heat conductivity on the $\Delta T(t)$ curve under the same Q_W also remained insignificant at the beginning of heating. For example, in the case of homogeneous heating in 1 cm^3 for $Q_w = 0$ the derivation $\mathrm{d}T/\mathrm{d}\lambda_x$ was constant, close to 0, in the first 15 s of heating and then decreased almost linearly in the next 2 min. This result has a simple analytical confirmation. Differentiation of equation (10) (Kučera *et al* 1977) at $t = 0$ gives $\frac{\mathrm{d}T}{\mathrm{d}t}(0) = \frac{P}{c_w \rho_w + c_x \rho_x}$, i.e., T is a function of the specific heat of moist wood (or wood water content) and independent of Q_W and λ. This is why $T'(0)$ can be used for the estimation of wood water content and, consequently, λ using the equations of Steinhagen (1977) relating λ with wood dry density and water content.

3.3. Analysis and simulation experiments with constant heating

3.3.1. Heat field pattern. Under $Q_W = 0$ the heat field of all arrangements was symmetric relatively to the horizontal plane crossing the middle of the heated domain. When Q_W increased the heat field stretched upwards from the heater, narrowed from the sides and its amplitude decreased. The results for the individual heating arrangements are described below.

Needle heating. All simulation experiments showed a very high temperature gradient close to the needle—ΔT usually dropped about three times within 5 mm from the needle; in contrast, under high sap flow values ΔT at 5 mm below the

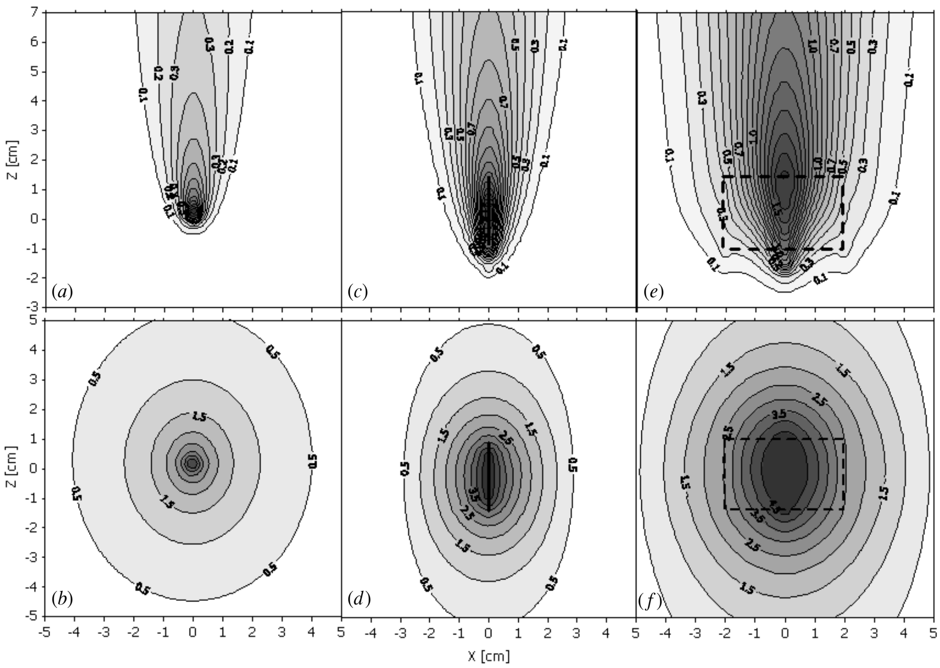

Figure 2. Typical configurations of simulated temperature field (tangential cross-section 1.5 cm from stem surface) for needle (*a*), (*b*), plate (*c*), (*d*) and volume (*e*), (*f*) heating for sap flow 0 (*a*), (*c*), (*e*) and 30 (*b*), (*d*), (*f*) g cm^{-2} h^{-1}. Bold segments (*c*), (*d*) and rectangles (e), (*f*) present heated domain.

needle approached 0 (figures 2(*a*) and (*b*)). The heat field under $Q_W = 0$ was significantly stretched along the z-axis due to the anisotropy of heat conductivity: the value of λ_z was up to 2.5 times higher compared to λ_x (Steinhagen 1977).

Heating by metallic plate. The typical temperature field for a 1 cm high copper heater is presented in figures 2(*c*) and (*d*). The tangential profile of ΔT (at the level of the heater) is characterized by the initial fall to about 10% to 20% mm^{-1}, which is significantly higher than for the volume heating, but much lower than for the needle heating.

Volumetric heating. The heat field under volume heating was wider and much more homogeneous than in the previous cases (figures 2(*e*) and (*f*)). The dramatic changes of the vertical temperature profile across the heated volume were observed even for a small increase of sap flow above zero. Under $Q_W = 0$ the vertical temperature profile was symmetric towards the horizontal plane across the middle of the heated volume (figure 3). For a small increase of Q_W ($0 < Q_W < 5$ g cm^{-2} h^{-1}) the vertical profile of ΔT first moved up a little and then acquired a typical form (see figure 3): $\Delta T \approx 0$ below the heated volume, it increased almost linearly within the heated volume, reaching a maximum at its top, and slowly decreased beyond it. The further increase of Q_W decreased ΔT, but the form of its vertical profile remained the same.

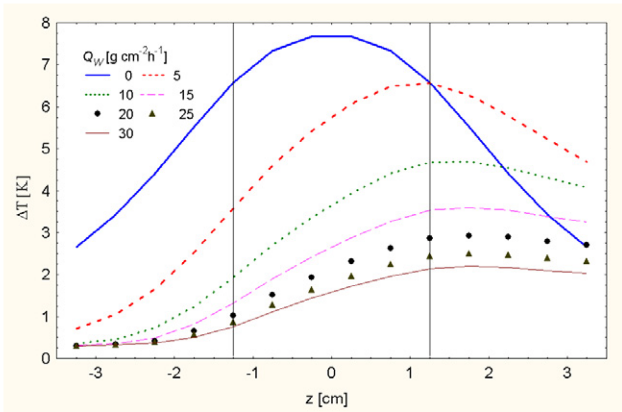

Figure 3. Homogeneous volume heating in 4 × 3 × 2.5 cm^3 by total power 0.63 W. $\lambda_x = 0.24$ W m^{-1} K^{-1}, $\lambda_z = 0.6$ W m^{-1} K^{-1}, no heat loss from bark. Vertical profile of ΔT for different values of sap flow along the line $x = 1$ cm and $r = 1.5$ cm. Vertical lines mark the limits of heated volume.

3.3.2. Dependence of Q_W on ΔT. All the configurations of heaters considered above showed a hyperbolic form of the dependence of Q_W on ΔT within or close to the heating element. It could be satisfactorily approximated ($r^2 > 0.99$) by the proposed types of equations ((10) for volume heating, (11) and (12)).

Specifically, equation (10) satisfactorily approximated the mentioned dependence for any variant of volume heating with and without heat loss from bark, when ΔT is measured anywhere in the central part of the heated volume, where it is relatively homogeneous and close to its maximum. Moreover, only the additive constant k reflecting the heat loss by heat conductivity should be estimated under $Q_W = 0$. This means that the zero-dimensional model of heat balance, based on equation (10), gives a reasonable approximation.

3.3.3. Sensitivity of ΔT to wood heat conductivity. Under any heating arrangements $\partial T/\partial\lambda$ had a maximum for $Q_W = 0$ and decreased with increasing Q_W, which reflects the decreasing portion of heat loss by conductivity in the total heat loss when heat convection by water flow increases. Dependence $\partial T/\partial\lambda$ was significantly non-linear, close to hyperbolic within the span of λ considered. For example, for a heated plate, $\partial T/\partial\lambda$

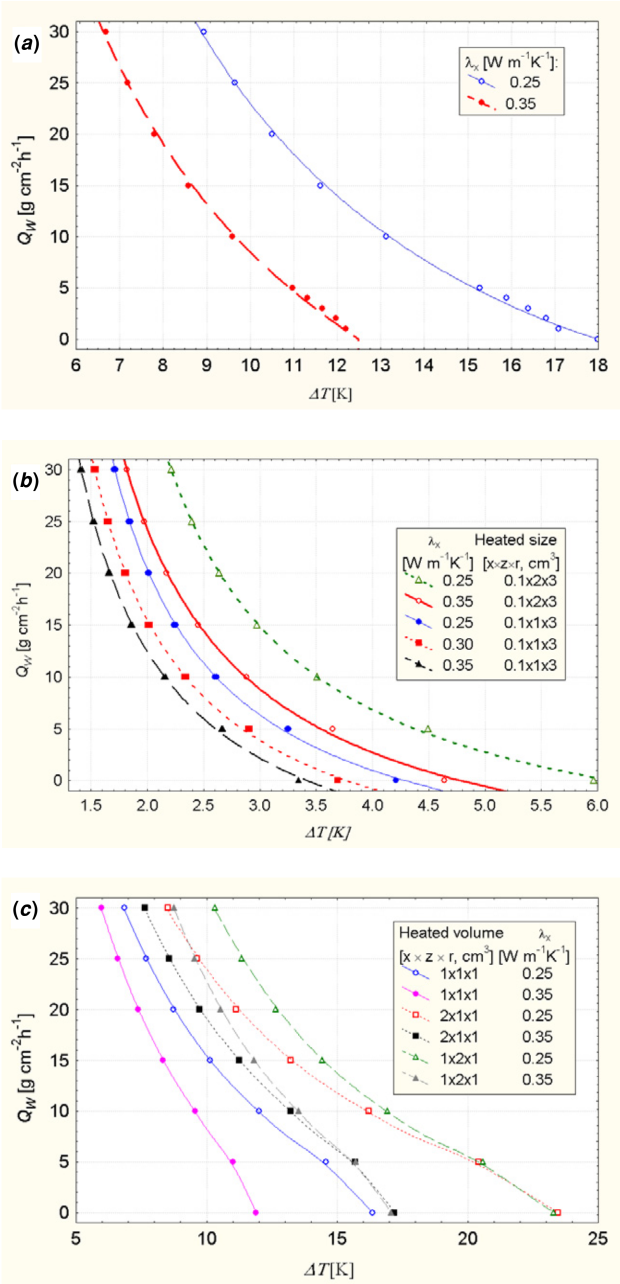

Figure 4. Simulated temperature dependence of sap flow for different heat conductivity of wood and size of heated domain ($x \times z \times r$) for needle (*a*), plate (*b*) and volume (*c*) heating ($\lambda_z = 2.5\lambda_x$).

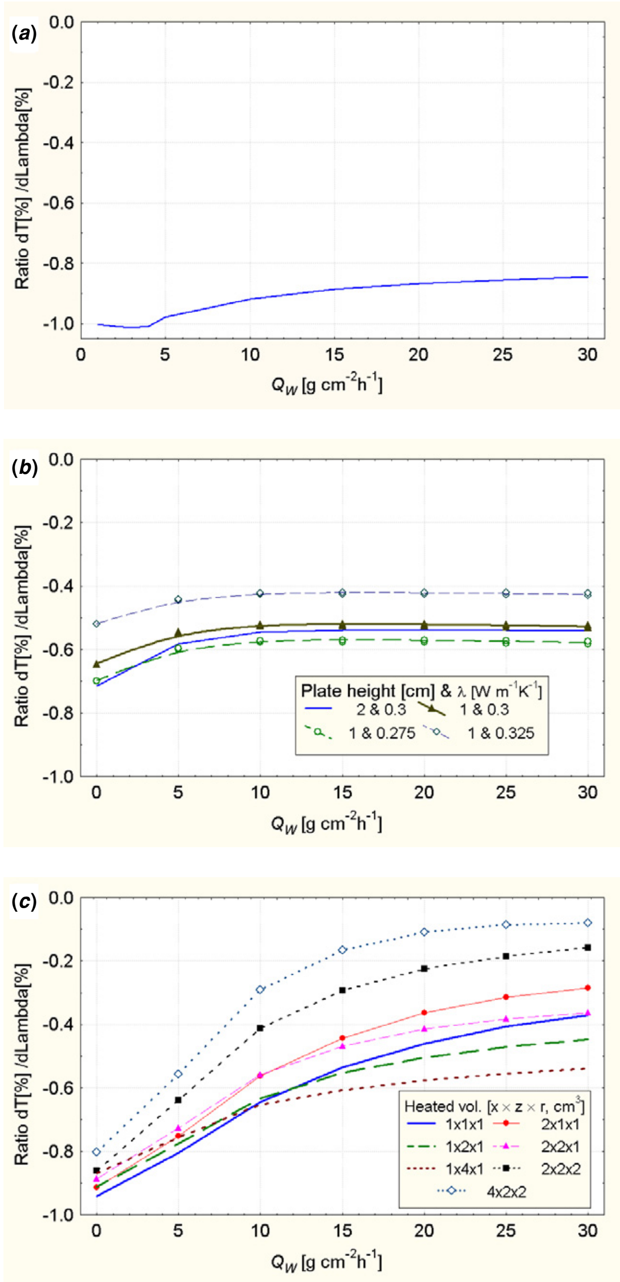

Figure 5. Dependence of simulated $\partial T/\partial\lambda$ (in per cent of dT to per cent of dλ) on sap flow for different sizes of heated domain ($x \times z \times r$) for needle (*a*), plate (*b*) and volumetric (*c*) heating.

was 1.5 times higher for $\lambda_x = 0.275$ W m^{-1} K^{-1}, than for $\lambda_x = 0.325$ W m^{-1} K^{-1}.

The simulation experiments with the needle heating showed a high sensitivity of ΔT within the heater to the heat conductivity of wood. Thus, the 40% change of λ evoked a 40% change of ΔT for $Q_W \leqslant 5$ g cm^{-2} h^{-1} and a 34% change for $Q_W \geqslant 25$ g cm^{-2} h^{-1} (figure 4(*a*) and figure 5(*a*)). In practice, this means that the changes of heat conductivity of the environment close to the needle (evoked in particular by a loose contact between the needle and wood) can significantly affect the needle temperature.

The sensitivity of ΔT to λ for a plate heater was significantly smaller than for needle heating (figure 4(*b*) and figure 5(*b*)). Thus, the same 40% increase of λ as in the previous case evoked for different Q_W decreased ΔT by 21% to 26% and 22% to 29% for 1 and 2 cm high heater plates, respectively. It means that the increase of the heater surface slightly increases the sensitivity to λ. $\partial T/\partial\lambda$ decreased from a maximum to a minimum for Q_W ranging from 0 to 10 g cm^{-2} h^{-1} and became constant for higher Q_W.

Under volume heating $\partial T/\partial\lambda$ was generally lower as compared to the other heating options, but showed a significantly higher dependence on Q_W (figure 4(*c*) and figure 5(*c*)). $\partial T/\partial\lambda$ decreased from 2.5 to 10 times for different sizes of heated domain when Q_W increased from 0 to 30 g cm^{-2} h^{-1}. The simulations of heating by a standard THB sensor taking into consideration the heat loss from bark showed for 40% increase of λ a decrease of ΔT from 0% to 23% for different Q_W. For high Q_W, ΔT became independent of heat conductivity. The increase of the heated volume generally led to a decrease in $\partial T/\partial\lambda$. Hence, under 40% increase of λ, spans of ΔT decrease within the considered span of Q_W (0–30 g cm^{-2} h^{-1}) were 15% to 37%, 6% to 34% and 3% to 32% for the heated volumes 1, 8 and 16 cm^3, respectively.

Decreasing $|\partial T/\partial\lambda|$ with increasing heated volume can be illustrated by the analysis of equation (2). In fact, the first two terms on its right-hand side correspond to the heat fluxes due to heat conductivity (q) and water flow (j), respectively. Let us consider the case of homogeneous heating in a parallelepiped V in the Cartesian coordinate system (x, z, r). The heat loss from the heated volume can be calculated as $\int_V [\nabla(\boldsymbol{\lambda}\nabla T) - \rho_w c_w (\mathbf{v}\nabla)T]\,\mathrm{d}\mathbf{x}$. According to the theorem of Gauss the $\int_V \nabla(\boldsymbol{\lambda}\nabla T)\,\mathrm{d}\mathbf{x} = \int_S \boldsymbol{\lambda}\nabla T\,\mathrm{d}\mathbf{n}$, where S is the surface of the heated space and $\mathbf{n}$ is the normal projection vector. As the vector $\mathbf{v}$ has only one vertical non-zero component $\rho_w v_z = Q_W$,

$$\int_V \rho_w c_w (\mathbf{v}\nabla)T\,\mathrm{d}\mathbf{x} = \int_A \mathrm{d}x \cdot \mathrm{d}r \int_{z_1}^{z_2} c_w Q_w \frac{\partial T}{\partial z}\,\mathrm{d}z$$

$$= \int_A c_w Q_w (T(z_2) - T(z_1)) \cdot \mathrm{d}x \cdot \mathrm{d}r,$$

where A is the horizontal cross-section of heated volume and z_1 and z_2 are z-coordinates of bottom and top boundaries of V. Under $Q_W \geqslant 5$ g cm^{-2} h^{-1} the temperature increases almost linearly from z_1 to z_2 (see figure 3). Thus, q is proportional to the surface area of the heated volume, whereas j is proportional to the heated volume. This is why under the same Q_W the increase of the heated volume leads to the decrease of the portion of heat loss by heat conductivity in the total heat loss from V, consequently to the decrease of $|\partial T/\partial\lambda|$.

Integration of equation (4) in 2D space (x- and z-coordinates) with heating in a rectangle area showed q to be proportional to the temperature at the centre of the heated area ($r^2 = 99.9\%$). The portion of q in the total heat loss decreased from 100% to 15% with increasing Q_W from 0 to 30 g cm^{-2} h^{-1}.

3.3.4. Effect of heterogeneity in sap flow radial profile. The aim of the following analysis is to examine whether the mean of the temperature radial profile can be applied to calculate sap flow in the whole profile. The theoretical analysis of this problem was done for the most simplified case similar to that considered by Kučera *et al* (1977). Let us suppose homogeneous heating in a parallelepiped with the power P per unit of depth insulated in the radial direction from both sides. Let us divide the heated volume into two parts A and B with completely homogeneous temperatures within each one and the depths R and r, respectively. Let us suppose sap flow within the heated width per unit depth $Q_{Wr} = Q_A$ in A and $Q_{Wr} = 0$ in B. Let us consider two extreme cases: (1) no heat flux between A and B, and (2) complete homogenization of temperature between A and B, i.e. infinite radial heat conductivity.

In case (1) we can directly apply equation (10) separately for A and B and solve it for the temperatures in A and B: $T_A = \frac{P}{c_w Q_A + \lambda_S}$ and $T_B = \frac{P}{\lambda_S}$, where λ_S (in W K^{-1} cm^{-1}) is the coefficient of heat loss per unit depth from the heated volume in the vertical and tangential directions. The mean temperature will be $T_{AB} = \left(\frac{P}{c_w Q_A + \lambda_S}R + \frac{P}{\lambda_S}r\right)\big/(R + r)$. Inserting T_{AB} in (10) and supposing homogeneous sap flow, we obtain the total water flow across the heated volume

$$Q_{WS} = \frac{Q_A R \cdot (R + r)\lambda_S}{c_w Q_A r + \lambda_S \cdot (R + r)}. \tag{13}$$

The actual water flow across the heated volume ($Q_{WS,a}$) is $Q_A R$. It is clear that Q_{WS} evaluated by (13) is always underestimated, $\lim_{Q_A\to 0} Q_{WS} = Q_A R$ and $\lim_{Q_A\to\infty} Q_{WS} = \frac{R}{r}\frac{\lambda_S}{c_w}(R + r)$. This is why under small Q_A the Q_{WS} evaluated by (13) is close to the actual one but with increasing Q_A the underestimation increases.

In the opposite case (2), supposing $T_A = T_B$, we can write simple differential equations similar to those presented in Kučera *et al* (1977), separately for volumes A and B,

$$T_A'(t) = R(P - Q_A c_w T_A(t) - \lambda_S T_A(t)) + q(t)$$

$$T_B'(t) = r(P - \lambda_S T_B(t)) - q(t)$$

where $q(t)$ is the heat flow between A and B. Taking into consideration that $T_A = T_B$, excluding $q(t)$ and solving the obtained differential equation for T_A, we obtain:

$$T_A(t) = \frac{P(R + r)}{c_w Q_A R + (R + r)\lambda_S} \times \left(1 - \exp\left(-\frac{t(c_w Q_A R + (R + r)\lambda_S)}{a_1(R + r)}\right)\right),$$

that gives in a steady state $T_A = \frac{P(R+r)}{c_w Q_A R + (R+r)\lambda_S}$ and according to (10) $Q_{WS} = (R + r)\left(\frac{P}{c_w T_A} - \frac{\lambda_S}{c_w}\right) = Q_A R$, i.e., under the given supposition Q_{WS} is predicted precisely for any R and r.

It becomes apparent that the homogenization of the radial temperature profile decreases the sensitivity of measurement of the total stem sap flow to the radial sap flow pattern. Therefore, it increases the measurement accuracy. In practice, this positive effect of temperature homogenization is evoked by heating elements with high heat conductivity extending in the radial direction. In contrast, the mean value of the temperature profile cannot give satisfactory results if this profile is heterogeneous due to radial sap flow pattern. The actual situation during practical measurements is usually somewhere between the two described extreme cases.

The numerical analysis of the effect of sap flow depth ($d_{\max}$) on the results of simulation for the plate heater showed (figure 6(*a*)) that the mentioned error in estimating Q_{WS} decreased with increasing Q_W (i.e., with decreasing ΔT), being negative (underestimation) for maximum Q_W and positive for Q_W close to 0. This error for a 1 cm high heater and $d_{\max}$ being 2/3, $\frac{1}{2}$ and 1/3 of d_h was, for $5 \leqslant Q_W \leqslant 30$ g cm^{-2} h^{-1}, within the intervals −8% to 15%, −10% to 20% and −8% to 30%, respectively. Similar results were obtained for a 2 cm high heater, too. Note that when $Q_W \to 0$ both Q_{WS} and $Q_{WS,0}$ are close to 0 and the estimation of error becomes useless. Thus, even under a sap flow depth of 1/3 of the heater depth the sensor based on a plate heater measures sap flow per unit stem circumference, i.e., the total stem sap flow, with acceptable accuracy.

The same analysis for volume heating (standard three-electrode THB sensor with heated volume by x, z and r being $40 \times 25 \times 30$ mm^3 showed the error for $d_{\max} = d_h/2$ and

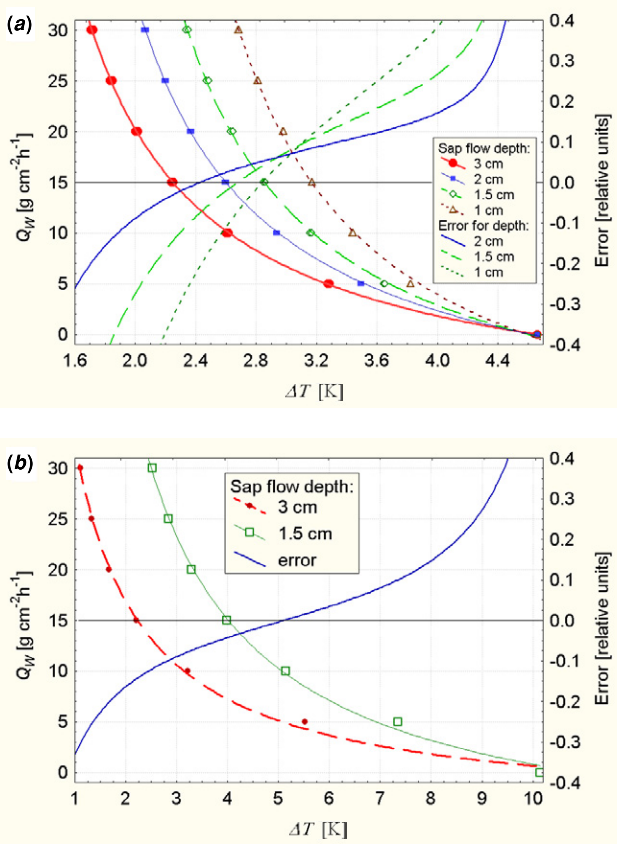

Figure 6. Simulated temperature dependence of sap flow for different sap flow depths and corresponding errors of calculation of sap flow total (see the text) for plate (*a*) and volume (*b*) heating. Heater depth is 3 cm in both cases.

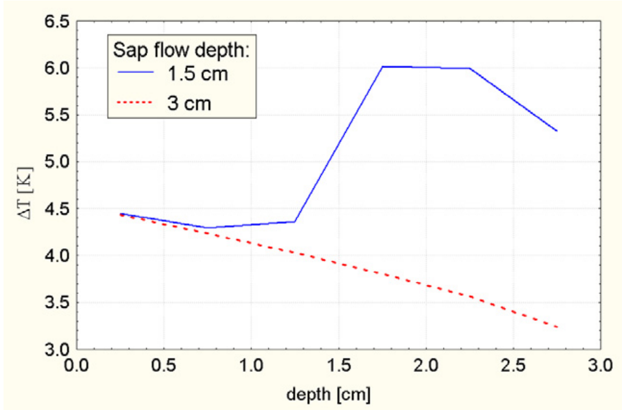

Figure 7. Needle heating. Simulated temperature along the needle for $Q_W = 30$ g cm^{-2} h^{-1} and sap flow depths 1/2 and whole needle depth.

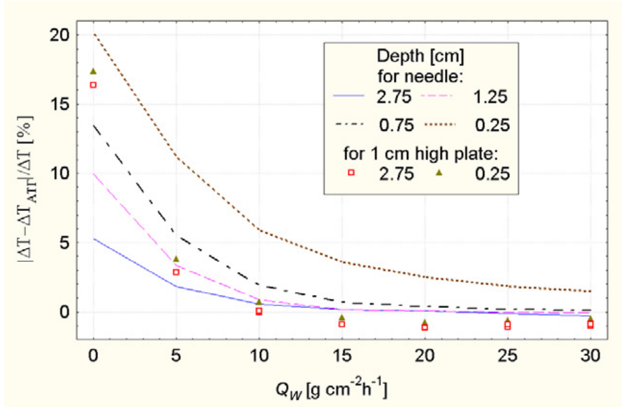

Figure 8. Needle and plate heating, heater depth 3 cm and sap flow depth 1.5 cm for both. Difference in heater ΔT simulated without and with the constant temperature difference of 2 K between stem surface and heartwood (in per cent of ΔT without gradient) at different depths in dependence on Q_W.

$5 \leqslant Q_W \leqslant 30$ g cm^{-2} h^{-1} from -10% to 9% figure 6(*b*)), which is slightly better than for a plate heater.

In contrast with volume and plate heating, where the radial temperature variations within the heated domain are almost completely homogenized by massive highly conductive heating elements, in the case of needle heating the needle temperature may vary remarkably with radius. Thus, for a 2 mm thick replete aluminium needle under high Q_W with $d_{\max} = d_h/2$ the temperature along the needle length can differ up to 2 times for depths less and higher than $d_{\max}$ (figure 7). This is why the above-considered error of estimation of Q_{WS} is strongly dependent on the depth of measurement and can reach hundreds of per cent if this depth is greater than $d_{\max}$.

3.3.5. Sensitivity of heat field on the radial temperature gradient. The simulations for an internally heated plate for sap depth $d_{\max} = d_h/2$ with and without ambient radial temperature gradient (ATG) gave very similar heater temperatures for $Q_W > 5$ g cm^{-2} h^{-1} differing by less than 1% (figure 8). However, under small sap flow, ΔT was higher when simulated without ATG compared to that simulated with ATG and this temperature excess rapidly increased with decreasing Q_W, showing 0.12 K (or 3.3%) for $Q_W = 5$ g cm^{-2} h^{-1} and 0.78 K (16.9%) for $Q_W = 0$.

The same simulations for needle heating gave a similar pattern of temperature difference along the needle without and with radial ATG (ΔT_G). Except for very shallow layer under the low sap flow condition, the effect of radial temperature difference is nearly negligible in both arrangements. However, when measuring the temperature difference between the reference and heated needle in a single depth, the measured value might be seriously affected by occasional differences in the sensor position. A similar error can be caused by a stem irregularity and consequent non-parallelism of bark surface and the isothermal surface.

Similar simulations with volume heating gave, for any Q_W, no significant difference between the temperature field obtained with and without temperature gradient.

3.4. Verification of simulation results by physical experiments

3.4.1. Evaluation of wood heat conductivity. Performed in spruce tree stems, the experiments to measure the dynamics of needle temperature under 1 min heating gave a geometrical mean of λ_z and λ_x driving the heat dissipation from the needle (see equation (9)) of 0.44 to 0.52 W m^{-1} K^{-1} for different experiments.

In the steady state of spruce, the comparison of the heat field around the needle with the simulated one for different values of λ_z and λ_x showed less anisotropy than that of 2.5 reported by Steinhagen (1977), namely about 1.7 ± 0.1. We obtained the best correlation ($r = 0.997$) between the model and the physical experiment for $\lambda_x = 0.45$ W m^{-1} K^{-1} and $\lambda_z = 1.6\lambda_x$. Therefore, the geometrical mean of λ_z and λ_x was very close to the result obtained from the above-mentioned dynamic measurements.

Similar experiments for an acacia segment gave the values of $\lambda_x = 0.27$ W m^{-1} K^{-1} and $\lambda_z = 2.5\lambda_x$, i.e., with the same ratio λ_z to λ_x as reported by Steinhagen (1977).

3.4.2. Comparison of simulated and measured temperature fields under $Q_W = 0$. The main problem in comparing the measured and simulated heat fields consists in the determination of the wood parameters applied in simulation, in particular λ_z, λ_x and the heat transfer coefficient of stem surface α.

In the case of the needle, the simulated temperature field was applied for the estimation of the heat conductivity as described above. When the obtained values of λ_z and λ_x were applied in simulations, the simulated temperature field closely matched the measured one ($r^2 \geqslant 0.99$).

For a volumetric heating with and without stem insulation, the measured and simulated vertical and horizontal temperature profiles across the heated segment were qualitatively similar. Quantitatively, measured profiles remained within the range obtained by simulation experiments (figure 9(*a*)). Similar results were obtained for plate heating, too. In practice, the determination of the bark insulation capacity of a living tree is difficult; therefore such a result is satisfactory. The best correlation between the simulated and measured vertical and horizontal temperature profiles ($r^2 = 0.98$–0.99) were obtained when no heat loss from the stem surface was taken into consideration (figure 9(*b*)).

3.5. Comparison of different types of sensors

3.5.1. Heat field pattern. The heat field in a steady state becomes more homogeneous as the heating domain becomes larger. The highest ΔT was observed for needle heating close to the heater, while ΔT was smaller for the plate heater and smallest for space heating.

3.5.2. Dependence of Q_W on ΔT. In general, all three heater configurations showed a hyperbolic dependence of Q_W on ΔT, which could be well approximated (with $r^2 > 0.99$) by different types of equations ((10) for volume heating, (11) and (12)). This means that $|\partial Q_W/\partial T|$ increases with decreasing ΔT, which means that the precision of calculation of Q_W from ΔT decreases. Two characteristics of the $Q_W(\Delta T)$ curve are important from the point of view of its applicability in practice: the ratio of ΔT for maximum to ΔT for zero sap flow and $|\partial Q_W/\partial T|$ for maximum Q_W. From this point of view, the volumetric heating appeared to be the most suitable because it had the maximal dynamics of relative ΔT ($\Delta T_{\mathrm{rel}} = \Delta T/\Delta T_{\max}$) corresponding to the considered dynamics of Q_W as well as the lowest $|\partial Q_W/\partial T|$ for the maximum Q_W (figure 10). The plate heater had the intermediate dynamics of ΔT between the volume and needle heating, but the maxima $|\partial Q_W/\partial T|$ for plate and for needle heaters were close to each other and about 1.5 higher compared to volume heating, i.e., needle and plate sensors are less sensitive to high Q_W compared to volumetric heating.

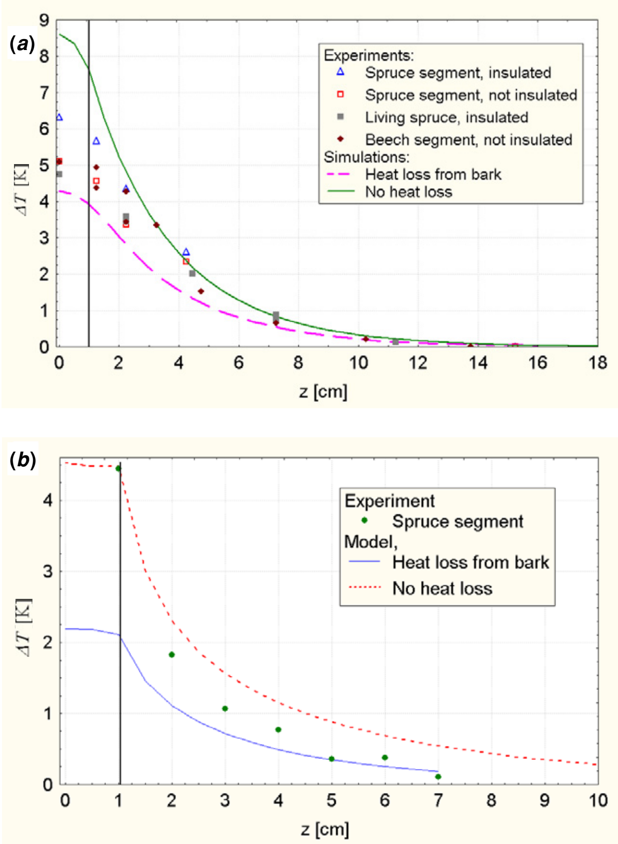

Figure 9. Simulated and measured vertical ΔT profiles through the middle of the heated domain for standard THB volume heating (*a*) and 2.5 cm high plate heating (*b*). Experiments were done on cut stem segments and leaving trees with and without insulation of the measuring point. Simulations were done with $\lambda_z = 0.756$ W m^{-1} K^{-1} and $\lambda_x = 0.42$ W m^{-1} K^{-1} measured for spruce (see the text). Vertical lines mark the limits of heated volume.

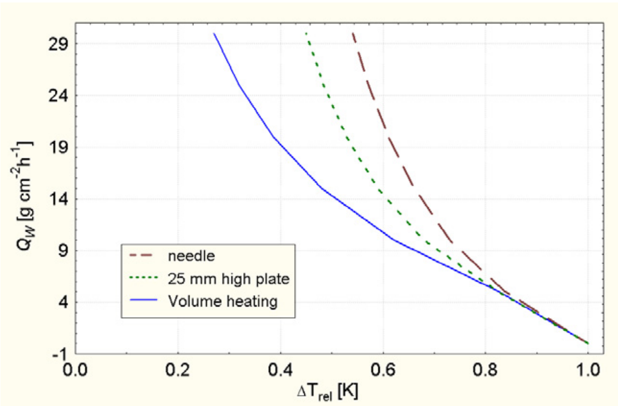

Figure 10. Dependence of sap flow on simulated ΔT related to maximum ΔT ($\Delta T_{\mathrm{rel}} = \Delta T/\Delta T_{\max}$) for different heating arrangements. ΔT is taken in the middle of the needle (plate, heated volume for standard THB volume heating). Simulations were done with heater depth 3 cm, $\lambda_z = 0.756$ W m^{-1} K^{-1} and $\lambda_x = 0.42$ W m^{-1} K^{-1} measured for spruce (see the text).

3.5.3. Effect of heat conductivity and heated volume on heat field. In general, enlargement of the horizontal projection of the heated domain (x and r axes) reduces the dependence of temperature field on wood heat conductivity (figure 5). The increase of the heated domain along the axis z (Z) has no significant effect for this dependence. Consequently, the highest dependence of ΔT on λ was observed for needle heating. Under volumetric heating, ΔT is sensitive to λ only under small sap flow conditions. A simple sensitivity calculation of Q_W using equation (10) showed that the high $|\partial T/\partial\lambda|$ under $Q_W \cong 0$ introduced a negligible error in Q_W estimation within the whole range of sap flow rate. Applying equation (10) for the actually measured ΔT and supposing 20% change of λ, the constant $\partial T/\partial\lambda$ as shown in the figure 5(a) resulted in a constant error of Q_W estimation of 15%, whereas under $|\partial T/\partial\lambda|$ decreasing with Q_W as shown in figure 5(c), this error varied from 1% to 3%.

3.5.4. Effect of sap flow radial profile on heat field. The sensitivity of temperature within a heated domain to the sap flow radial non-homogeneity depends on the massiveness and heat conductivity of heating (sensing) elements. This is why the needle heater is the most sensitive to the Q_W radial profile giving practically senseless results when temperature is measured at only one point of a heterogeneous sap flow profile. This means that the sap flow radial profile should be known for such sensor types (Kostner *et al* 1998). In contrast, in the case of heaters composed of metallic plates (plate and volumetric heating by electrodes) that significantly homogenize the temperature along them, the satisfactory approximation of sap flow per unit stem circumference (Q_{WS}) was reached even for sap flow occurring at 1/3 of the heater depth in the radial direction.

3.5.5. Effects of radial temperature gradient on heat field. The ΔT field for needle and plate heaters, in particular the heater ΔT, was significantly affected by radial ATG only under small sap flow and close to the stem surface. The temperature field under volume heating was not affected by ATG under any sap flow rate.

4. Conclusions

(1) The dependence of Q_W on ΔT at a certain point inside the heated domain for all considered configurations of heating can be satisfactorily (with $r^2 \geqslant 0.99$) approximated by various curves of hyperbolic type.
(2) The sensitivity of the temperature field in wood to all uncertainty factors decreases with the size of the heated domain. Thus, the sap flow sensor based on the needle heating is very sensitive to these factors, including wood heat conductivity, sap flow radial profile and temperature gradients, as well as the exact position of sensing elements if the temperature is measured in the wood close to the needle.
(3) The dependence of ΔT at a certain point on λ decreases with increasing horizontal projection of the heated domain and with increasing sap flow. It is maximal for a needle and negligible for a standard THB sensor, except for the case of small sap flow rate. The sensitivity of $\partial T/\partial\lambda$ to sap flow decreases with increasing vertical size of the heated domain.
(4) The increasing size (volume) of the heated domain increases the power consumption, time of reaching steady state, the minimal size of sample stem and (for some sensor configurations such as THB) necessary operator skills.
(5) The zero-dimensional heat balance model as applied by Kučera *et al* (1977) proved to be a satisfactory approximation for different arrangements of volume heating; i.e., equation (10) derived from this model gives a reasonable physically based approximation of sap flow.

Acknowledgments

The study was supported by Environmental Measuring Systems Inc., Brno, Czech Republic. The authors express their best thanks to Drs Michael Lashkevich and Nikolay Sysuyev for their very helpful consultation in theoretical physics and programming.

References

Cermak J, Cienciala E, Kučera J, Lindroth A and Hallgren J-E 1992 Radial velocity profiles of water flow in stems of spruce and oak and response of spruce tree to severing *Tree Physiol.* **10** 367–80

Cermak J, Deml M and Penka M 1973 A new method of sap flow rate determination in trees *Biol. Plant.* **15** 171–8

Cermak J, Kučera J and Stepankova M 1991 Water consumption of full-grown oak (*Quercus robur* L.) in a floodplain forest after the cessation of flooding *Floodplain Forest Ecosystem II (Developments in Agriculture and Managed Forest Ecology* 15B*)* ed M Penka, M Vyskot, E Klimo and F Vasicek (Amsterdam: Elsevier) pp 397–417

Cermak J, Ulehla J, Kučera J and Penka M 1982 Sap flow rate and transpiration dynamics in the full-grown oak (*Quercus robur* L.) in floodplain forest exposed to seasonal floods as related to potential evapotranspiration and tree dimensions *Biol. Plant.* **24** 446–60

Clearwater M J, Meinzer F C, Andrade J L, Goldstein G and Hallbrook N M 1999 Potential errors in measurement of nonuniform sap flow using dissipation probes *Tree Physiol.* **19** 681–7

Granier A 1985 Une nouvelle méthode pour la mesure du flux de sève brute dans le tronc des arbres *Ann. For. Sci.* **42** 193–200

Herrington L P 1969 *On Temperature and Heat Flow in Tree Stems* (New Haven, CT: Yale University Press) p 80

Huber B and Schmidt E 1936 Weitere thermoelektrische Untersuchungen uber den Transpirationsstrom der Baume *Thar. Forstl. Jb.* **87** 369–412

Kostner B, Granier A and Cermak J 1998 Sapflow measurements in forest stands: methods and uncertainties *Ann. Sci. For.* **55** 13–27

Kučera J, Cermak J and Penka M 1977 Improved thermal method of continual recording the transpiration flow rate dynamics *Biol. Plant. (Praha)* **19** 413–20

Kuna L 1959 *The Manual for Insulators of Heat and Moisture* (Bratislava) p 223 (in Slovak)

Lundblad M, Lagergren F and Lindroth A 2001 Evaluation of heat balance and heat dissipation methods for sapflow measurements in pine and spruce *Ann. For. Sci.* **58** 625–38

Phillips N, Oren R and Zimmermann R 1996 Radial patterns of xylem sap flow in non-, diffuse- and ring-porous tree species *Plant Cell Environ.* **19** 983–90

Rokitta M, Peuke A, Zimermann U and Haase A 2003 Spatially and temporally resolved measurement of xylem and phloem flow by NMR micro-imaging *Proc. 5th Int. Workshop 'Plant Water Relations and Sap Flux Measurements' (Firenze, 9–10 Nov. 2000)* ed R Tognetti and A Raschi pp 195–201

Sakuratani T 1981 A heat balance method for measuring water flux in the stem of intact plants *J. Agric. Met. (Japan)* **37** 9–17

Schubert H 1999 Qualitative und quantitative Untersuchung verschiedener Methoden der Xylemflussmessung an Baumen *PhD Thesis* Ludwig Maximilians University, Munchen, p 102

Siau J F 1984 *Transport Processes in Wood* (Berlin: Springer) p 245

Steinhagen P 1977 Thermal conductive properties of wood, green and dry, from −40 °C to +100 °C; literature review *USDA Forest Service General Technical Report FLP-9*

Swanson R H 1967 Seasonal course of transpiration of lodgepole pine and engelmann spruce *For. Serv. Rep.* 419–34

Swanson R H 1994 Significant historical development in thermal methods for measuring sap flow in trees *Agric. For. Meteorol.* **72** 113–32

Zimmerman M H 1983 *Xylem Structure and the Ascent of Sap* (Berlin: Springer) p 143